mathematics

IMPACT FACTOR 2.2

CITESCORE 4.6

Article

Scalar Field and Quintessence in Late-Time Cosmic Expansion

Aroonkumar Beesham

MDPI

https://doi.org/10.3390/math13243917

mathematics

MDPI

Article

Scalar Field and Quintessence in Late-Time Cosmic Expansion

Aroonkumar Beesham [1,2,3,4]

[1] Department of Mathematical Sciences, University of Zululand, P Bag X1001, Kwa-Dlangezwa 3886, South Africa; beeshama@unizulu.ac.za
[2] Faculty of Applied and Health Sciences, Mangosuthu University of Technology, Durban 4000, South Africa
[3] National Institute for Theoretical and Computational Sciences (NITheCS), Stellenbosch 7613, South Africa
[4] DSTI-NRF Centre of Excellence in Mathematical and Statistical Sciences (CoE-MaSS), Johannesburg 2001, South Africa

Abstract

The persistent Hubble tension—marked by a notable disparity between early- and late-universe determinations of the Hubble constant H_0—poses a serious challenge to the standard cosmological framework. Closely linked to this is the $H_0 - r_d$ tension, which stems from the fact that BAO-based estimates of H_0 are intrinsically dependent on the assumed value of the sound horizon at the drag epoch, r_d. In this study, we construct a scalar field dark energy model within the framework of a spatially flat Friedmann–Lemaitre–Robertson–Walker model to explore the dynamics of cosmic acceleration. To solve the field equations, we introduce a generalized extension of the standard Lambda Cold Dark Matter model that allows for deviations in the expansion history. Employing advanced Markov Chain Monte Carlo techniques, we constrain the model parameters using a comprehensive combination of observational data, including Baryon Acoustic Oscillations, Cosmic Chronometers, and Standard Candle datasets from Pantheon, Quasars, and Gamma-Ray Bursts (GRBs). Our analysis reveals a transition redshift from deceleration to acceleration at $z_{\rm tr} = 0.69$ and a present-day deceleration parameter value of $q_0 = -0.64$. The model supports a dynamical scalar field interpretation, with an equation of state parameter satisfying $-1 < \omega_0^{\phi} < 0$, consistent with quintessence behavior, and signaling a deviation from the Λ. While the model aligns closely with the Lambda Cold Dark Matter scenario at lower redshifts ($z \lesssim 0.65$), notable departures emerge at higher redshifts ($z \gtrsim 0.65$), offering a potential window into modified early-time cosmology. Furthermore, the evolution of key cosmographic quantities such as energy density ρ^{ϕ}, pressure p^{ϕ}, and the scalar field equation of state highlights the robustness of scalar field frameworks in describing dark energy phenomenology. Importantly, our results indicate a slightly higher value of the Hubble constant H_0 for specific data combinations, suggesting that the model may provide a partial resolution of the current H_0 tension.

Keywords: dark energy; late-time acceleration of universe; scalar field; quintessence

MSC: 83F05

Academic Editor: Leonid Piterbarg

Received: 21 October 2025
Revised: 27 November 2025
Accepted: 5 December 2025
Published: 7 December 2025

Citation: Beesham, A. Scalar Field and Quintessence in Late-Time Cosmic Expansion. *Mathematics* **2025**, *13*, 3917. https://doi.org/10.3390/math13243917

1. Introduction

Einstein's theory of General Relativity (GR) has stood as the foundational framework of gravitational physics and modern cosmology, providing remarkably accurate predictions across a wide range of astrophysical and cosmological phenomena. From the precession of Mercury's perihelion and the deflection of light by massive bodies, to the precise modeling

of gravitational lensing and the large-scale dynamics of galaxy clusters, GR has withstood over a century of rigorous experimental and observational scrutiny. Despite its success, applying GR to the universe at cosmological scales reveals profound limitations. Most notably, GR alone cannot account for the observed accelerated expansion of the universe without introducing an exotic energy component with negative pressure—commonly termed dark energy. This enigmatic form of energy, inferred primarily from observations of Standard Candle (SNe Ia) datasets, Cosmic Microwave Background (CMB) anisotropies, and Baryon Acoustic Oscillations (BAOs), remains one of the deepest mysteries in theoretical physics and cosmology [1–3]. These challenges have motivated the exploration of extended theories of gravity and alternative cosmological models that go beyond the standard Lambda Cold Dark Matter (ΛCDM) model paradigm.

Observational data from multiple independent cosmological probes—including SNe Ia, CMB anisotropies, and BAO—have firmly established that the universe is undergoing a phase of accelerated expansion. Within the framework of the standard ΛCDM model, this acceleration is attributed to a Λ, often interpreted as the vacuum energy density with a constant equation of state (EoS) $\omega = -1$. Despite the success of the ΛCDM model in fitting a broad range of cosmological data, growing tensions between early- and late-time measurements of key parameters, most notably of the Hubble constant (H_0) and of the sound horizon scale at the drag epoch (r_d), have called into question the completeness of this model. This so-called Hubble tension reflects a significant discrepancy between the local (late-universe) measurements of H_0, such as those based on Cepheid-calibrated SNe Ia, and the value inferred from the CMB under ΛCDM assumptions. Similarly, the $H_0 - r_d$ tension, emerging from BAO data, suggests possible inconsistencies in the assumed physics of the early universe. These anomalies have motivated increasing interest in alternative cosmological models and modifications to GR that go beyond the standard paradigm.

Early-universe estimates, particularly those derived from Planck CMB data under the standard ΛCDM framework, favor a lower value of H_0 [3]. In contrast, local measurements based on the Cepheid-calibrated distance ladder, such as those by Riess et al., yield significantly higher values [4,5]. This discrepancy, now exceeding the 5σ threshold in some analyses, has sparked debate about whether the cause lies in unresolved systematic uncertainties or points to the need for new physics beyond the standard cosmological model.

Closely linked to this is the $H_0 - r_d$ tension, which arises due to the dependence of Baryon Acoustic Oscillation (BAO)-based determinations of H_0 on the sound horizon at the drag epoch, r_d. In the standard approach, r_d is calculated from early-universe physics assuming well-established pre-recombination conditions. However, recent investigations suggest that modifying early expansion dynamics, introducing additional relativistic species, or altering the gravitational sector could change the value of r_d, thereby affecting BAO-based estimates of H_0 [6,7]. This interconnected set of tensions points to potential gaps in our theoretical understanding of the cosmic expansion history and motivates ongoing exploration of alternative cosmological models.

In the quest to explain the late-time accelerated expansion of the universe, modified gravity theories (MGTs) have emerged as compelling alternatives to the standard ΛCDM paradigm, which relies on a Λ. These MGTs modify the geometric sector of Einstein's field equations and allow for cosmic acceleration without invoking dark energy in the form of a constant vacuum energy density. One of the most well-studied frameworks is $f(R)$ gravity, where the Ricci scalar R in the Einstein–Hilbert action is replaced with a generic function $f(R)$ [8–10]. This extension naturally leads to accelerated expansion under certain functional forms of $f(R)$ and has been successfully tested in various cosmological settings. Similarly, $f(T)$ gravity modifies the gravitational action by replacing curvature with torsion (T), as formulated in the teleparallel equivalent of GR [11,12]. Other

extensions include $f(R,T)$ gravity, where T denotes the trace of the energy-momentum tensor, introducing explicit matter–geometry coupling [13], and $f(R,L_m)$ gravity, where the Lagrangian density of matter L_m interacts with curvature, enabling novel gravitational dynamics [14]. More recently, $f(Q)$ gravity, based on the non-metricity scalar Q, has garnered attention for its ability to describe cosmological acceleration within the symmetric teleparallel framework [15,16]. Further generalization is achieved in $f(Q,T)$ gravity, where both non-metricity and matter contribute non-trivially to the gravitational Lagrangian [17].

Scalar–tensor theories constitute a wide family of models where a dynamical scalar field is coupled to gravity. The most general second-order scalar–tensor theory is the Horndeski theory [18], which accommodates a rich set of interactions capable of producing late-time cosmic acceleration without introducing Ostrogradsky instabilities. Subsequent developments, known collectively as beyond-Horndeski or degenerate higher-order scalar–tensor (DHOST) theories [19], extended the Horndeski class while maintaining stability through specific degeneracy conditions.

Whilst these frameworks are extremely general, they encompass a large number of free functions and couplings, making them powerful but difficult to constrain fully without strong theoretical priors and extensive datasets. In contrast, the present work focuses on a minimal and phenomenological scalar-field extension of the ΛCDM model, constructed directly at the level of the background expansion. Our model does not attempt to explore the full Horndeski or DHOST function space; rather, it provides a controlled, observationally driven deviation from the ΛCDM model that retains compatibility with standard scalar-field dynamics. This allows us to focus on the cosmological consequences of a dynamical equation-of-state evolution without invoking the broader complexity of the full Horndeski class.

Nevertheless, our approach is complementary to Horndeski and beyond-Horndeski studies. Many subclasses of Horndeski theories reduce effectively to a canonical or non-canonical scalar field with a modified expansion history at the background level. The generalized $H(z)$ extension introduced in our work can therefore be viewed as a simplified effective description of a wider class of scalar–tensor theories, capturing their key phenomenological signatures while remaining tractable for joint MCMC analysis with multiple datasets. Hence, the main feature of our model is its simplicity.

Parallel to these geometric modifications, scalar field cosmologies provide another well-motivated class of models for understanding both the present cosmic acceleration and the early inflationary epoch [20,21]. In these models, a scalar field ϕ evolves dynamically and interacts with the geometry of spacetime. The associated potential $V(\phi)$ is responsible for producing negative pressure, thereby driving accelerated expansion [20–23]. Among these, the quintessence model is a widely studied scalar field framework that proposes a slowly rolling scalar field as the source of dark energy. It offers significant theoretical advantages, particularly in addressing the fine-tuning and cosmic coincidence problems [22,23]. Unlike a Λ, quintessence permits the energy density of dark energy to vary with time, thus reducing the need for unnatural initial conditions. The evolution of the scalar field may be guided by specially designed potentials, allowing its energy density to naturally approach that of matter at late times, offering a dynamic solution to the coincidence problem. A crucial concept within the quintessence framework is that of tracker fields, introduced in [24], where the scalar field evolves along an attractor solution largely independent of initial conditions. This tracking behavior has received substantial observational support and enhances the model's predictive power. The literature further explores extended quintessence models, including those with non-minimal coupling between the scalar field and gravity [25,26] and those involving non-canonical kinetic terms, such as k-essence or tachyonic fields [27]. The role of time-dependent EoS parameters in

scalar–tensor theories has been rigorously examined, offering rich phenomenology in both background dynamics and structure formation [28,29]. Moreover, scalar fields are not limited to cosmological applications. They also play important roles in various astrophysical processes, such as black hole physics, stellar structure, and compact object dynamics. This broad applicability has led to the proliferation of scalar field–based models across both theoretical and observational domains [28–33].

A comprehensive investigation of dynamical dark energy models and MGTS is essential, especially in the context of current and future high-precision cosmological observations. The complex and still poorly understood mechanisms responsible for the late-time acceleration of the universe necessitate rigorous theoretical scrutiny and empirical validation. To facilitate such studies, numerous parametrizations have been developed to effectively describe the evolution of key cosmological quantities, including the Hubble parameter, deceleration parameter, and EoS parameter [34–37]. These parametrizations serve as powerful tools for testing the viability of competing models against observational datasets.

Building on the broader framework of dynamical cosmology, this study adopts a specific parametrization of the Hubble parameter $H(a)$, designed as a generalization to the ΛCDM model. By introducing a physically motivated yet flexible functional form for $H(a)$, we aim to capture the key features of cosmic expansion in a manner that allows direct confrontation with observational data. To place robust constraints on the model, we utilize a comprehensive suite of cosmological datasets, including BAO, CC, and SNe Ia from the Pantheon compilation, complemented by measurements from quasars and GRBs. These diverse observational probes offer independent measurements of the Hubble parameter $H(z)$, enabling a detailed reconstruction of the cosmic expansion history and precise constraints on the deceleration parameter and related cosmological quantities. We perform a thorough statistical analysis using Markov Chain Monte Carlo techniques to explore the parameter space and derive the posterior distributions of the model parameters. A Gaussian prior on the Hubble constant H_0, based on the measurement in [38] is incorporated to investigate potential tensions between early- and late-time cosmological constraints. Additionally, a covariance matrix analysis is carried out to rigorously account for correlations within the observational datasets, thereby ensuring the statistical robustness and reliability of the inferred cosmological parameters.

The structure of this paper is as follows. In Section 2, we provide the field equations, and, in Section 3, we introduce our parametrization of the Hubble parameter. The confrontation of the model against observations is performed in Section 4. In Section 5, we discuss the cosmographic parameters, and, in Section 6, the evolution of the scalar field is elucidated upon, with its relevance to quintessence. Finally Section 7 provides our concluding remarks.

2. Field Equations

Unveiling the true nature of dark energy remains one of the most formidable challenges in modern cosmology. Although the Λ provides a phenomenological explanation for the observed acceleration of the universe, its theoretical limitations, notably the fine-tuning and coincidence problems, have motivated the exploration of dynamic alternatives. Among these, quintessence, a canonical scalar field slowly evolving in time, has emerged as a compelling and theoretically rich candidate for dark energy.

The action for a scalar field minimally coupled to gravity, as proposed in [39], is given by

$$S = \int d^4x \sqrt{-g}\left(\frac{1}{2}M_{\rm Pl}^2 R + \mathcal{L}_m + \mathcal{L}_\phi\right), \tag{1}$$

where $\mathcal{L}_m$ denotes the Lagrangian for ordinary matter, and $\mathcal{L}_\phi$ represents the scalar field Lagrangian, defined as

$$\mathcal{L}_\phi = -\frac{1}{2} g^{ij} \partial_i \phi \, \partial_j \phi - V(\phi). \tag{2}$$

In this formulation, g is the determinant of the metric tensor g_{ij}, $M_{\rm Pl} = (8\pi G)^{-1/2}$ is the reduced Planck mass, R is the Ricci scalar, and $V(\phi)$ is the scalar potential responsible for the self-interaction of the field. For physically viable models, the scalar field ϕ is typically assumed to be positive definite. Within the context of dark energy phenomenology, models are broadly categorized as either interacting or non-interacting. Interacting models involve energy exchange between dark energy and cold dark matter [40–42], while non-interacting models assume the independent evolution of matter and dark energy components [43–45]. In this work, we consider a minimally coupled quintessence scenario.

In Equation (1), we have presented the Einstein–Hilbert action minimally coupled to a scalar field. Formally, the Einstein–Hilbert action requires the inclusion of the Gibbons–Hawking–York (GHY) boundary term in order to ensure a well-posed variational principle. The complete gravitational action should therefore be written as

$$S_{\rm grav} = \frac{1}{2} M_{Pl}^2 \int d^4x \, \sqrt{-g} \, R + S_{\rm GHY}, \tag{3}$$

where

$$S_{\rm GHY} = \frac{M_{Pl}^2}{8\pi} \int_{\partial \mathcal{M}} d^3x \, \sqrt{|h|} \, K \tag{4}$$

is the standard boundary contribution, with h denoting the induced metric on the boundary $\partial \mathcal{M}$ and K the trace of the extrinsic curvature.

In the present work, we do not explicitly include the boundary term because, in a Friedmann–Lemaitre–Robertson–Walker (FLRW) spacetime, the GHY term reduces to a total derivative and does not contribute to the field equations. Under the usual assumptions such as spatial hypersurfaces without boundary or negligible contributions at temporal boundaries, the boundary term vanishes. Therefore, omitting it does not affect the Einstein equations or the scalar-field dynamics obtained from Equation (1). This treatment follows standard practice in cosmological analyses involving minimally coupled scalar fields.

Varying the action (1) with respect to the metric yields the Einstein field equations:

$$R_{ij} - \frac{1}{2} R g_{ij} = M_{\rm Pl}^{-2} T_{ij}^{(\rm tot)}, \tag{5}$$

where the total energy-momentum tensor is given by the sum of the matter and scalar field contributions:

$$T_{ij}^{(\rm tot)} = T_{ij}^{(m)} + T_{ij}^{(\phi)}. \tag{6}$$

The energy-momentum tensor corresponding to the scalar field ϕ is expressed as

$$T_{ij}^{(\phi)} = \partial_i \phi \, \partial_j \phi - \frac{1}{2} g_{ij} (\partial \phi)^2 - g_{ij} V(\phi), \tag{7}$$

where $(\partial \phi)^2 \equiv g^{ij} \partial_i \phi \, \partial_j \phi$. The scalar field also satisfies the Klein–Gordon equation:

$$\nabla^i \nabla_i \phi - \frac{dV}{d\phi} = 0. \tag{8}$$

To model the large-scale geometry of the universe, we adopt the spatially homogeneous and isotropic FLRW metric:

$$ds^2 = -dt^2 + a(t)^2\left(\frac{dr^2}{1-kr^2} + r^2 d\theta^2 + r^2 \sin^2\theta\, d\phi^2\right), \tag{9}$$

where $a(t)$ is the scale factor, and $k = +1, 0, -1$ corresponds to closed, flat, and open spatial curvature, respectively. Observations favor a spatially flat geometry ($k = 0$), reducing the metric to

$$ds^2 = -dt^2 + a(t)^2\left(dr^2 + r^2 d\theta^2 + r^2 \sin^2\theta\, d\phi^2\right). \tag{10}$$

Within this background, the Einstein field equations simplify to the Friedmann equations:

$$3H^2 = M_{\rm Pl}^{-2}\rho^{(\rm tot)}, \tag{11}$$

$$(2q-1)H^2 = M_{\rm Pl}^{-2}p^{(\rm tot)}, \tag{12}$$

where $H = \dot{a}/a$ is the Hubble parameter, and $q = -\ddot{a}/\dot{a}^2$ is the deceleration parameter. The total energy density and pressure are the sum of the matter and scalar field contributions:

$$\rho^{(\rm tot)} = \rho^{(m)} + \rho^{(\phi)}, \quad p^{(\rm tot)} = p^{(m)} + p^{(\phi)}. \tag{13}$$

The energy density and pressure associated with the scalar field are given by

$$\rho^{(\phi)} = \frac{1}{2}\dot{\phi}^2 + V(\phi), \quad p^{(\phi)} = \frac{1}{2}\dot{\phi}^2 - V(\phi), \tag{14}$$

where $\frac{1}{2}\dot{\phi}^2$ and $V(\phi)$ represent the kinetic and potential energies of the scalar field, respectively. The effective EoS parameter for the scalar field is then defined as

$$\omega^{(\phi)} = \frac{p^{(\phi)}}{\rho^{(\phi)}} = \frac{\frac{1}{2}\dot{\phi}^2 - V(\phi)}{\frac{1}{2}\dot{\phi}^2 + V(\phi)}. \tag{15}$$

In contrast to the Λ ($\omega = -1$), the EoS parameter for quintessence evolves dynamically within the range $-1 < \omega^{(\phi)} < 0$. A value closer to -1 indicates potential-dominated evolution, mimicking Λ, whereas kinetic dominance leads to higher values of $\omega^{(\phi)}$, resulting in weaker acceleration. The total energy-momentum conservation law, derived from Equations (11) and (12), is given by

$$\dot{\rho}^{(\rm tot)} + 3H\left(\rho^{(\rm tot)} + p^{(\rm tot)}\right) = 0. \tag{16}$$

Finally, using Equations (11) and (14), we can isolate the kinetic and potential components of the scalar field in terms of cosmological parameters:

$$\dot{\phi}^2 = 2M_{\rm Pl}^2(q+1)H^2 - \rho^{(m)}, \tag{17}$$

$$V(\phi) = M_{\rm Pl}^2(2-q)H^2 - \frac{1}{2}\rho^{(m)}. \tag{18}$$

These relations allow a reconstruction of the scalar field dynamics based on observational constraints on $H(z)$, $q(z)$, and $\rho^{(m)}(z)$. The mathematical expressions used in the paper describe well-established physical ideas behind cosmic acceleration and dynamical dark energy. The parametrized expansion history $H(z)$ is interpreted as arising from a time-evolving scalar field whose energy density and pressure determine the universe's acceleration. The scalar field's kinetic and potential energies naturally lead to a redshift-dependent EoS $w_\phi(z)$, offering richer physical behaviour than a constant Λ.

The derived quantities $\rho_\phi(z)$, $p_\phi(z)$, $w_\phi(z)$, and $q(z)$ represent how the scalar field competes with matter and eventually dominates, leading to the transition from deceleration

to acceleration at $z_{tr} = 0.69$. This transition is a physically meaningful stage when dark energy overtakes matter. The early-time deviations in $H(z)$ produced by the model influence the sound horizon scale r_d, allowing a higher inferred value of H_0 and offering a physically motivated pathway toward alleviating the Hubble tension. Finally, the combination of CC, BAO, SNe Ia, QSOs, and GRBs datasets provides a coherent physical test of the model across cosmic time by linking expansion history, distance measures, and early-universe imprints.

3. Parametrization of Hubble Parameter

Parametrizations play a pivotal role in probing the nature of the dark energy-dominated universe in a model-independent framework. By formulating suitable functional forms of key cosmological quantities such as the Hubble parameter or the deceleration parameter, and confronting them with observational data, one can effectively discriminate between viable and non-viable cosmological scenarios. In order to get definite solutions, it is often necessary to introduce such parametrizations. This approach offers a flexible and theoretically agnostic path to understanding late-time cosmic acceleration.

In this work, we adopt a generalized parametric form of the Hubble parameter as a function of the scale factor $a(t)$, given by

$$H(a) = H_0\sqrt{\alpha\, a^{-\beta} + (1-\alpha)}, \tag{19}$$

where α and β are free model parameters. This formulation generalizes the standard ΛCDM Hubble, which is

$$H(a) = H_0\sqrt{\Omega_m a^{-3} + \Omega_\Lambda},$$

and accommodates a broader range of cosmological behaviors, depending on the values of β. Parametrizations like Equation (19) have been widely employed in the literature to explore alternatives to the ΛCDM model in both standard and modified gravity scenarios [46–51].

Transforming Equation (19) into a redshift-based formulation using the relation $a = \frac{1}{1+z}$ (with $a_0 = 1$ for the present epoch), we obtain

$$H(z) = H_0\sqrt{\left[\alpha(1+z)^{\beta} + (1-\alpha)\right]}. \tag{20}$$

To understand the dynamics of cosmic expansion, the cosmographic parameters, particularly the deceleration parameter q, provide crucial insight. This parameter helps classify different epochs of cosmic evolution: $q > 0$ signifies a decelerated phase, $-1 < q < 0$ corresponds to power-law acceleration, $q = -1$ denotes exponential (de Sitter) expansion, and $q < -1$ indicates a super-exponential regime. The deceleration parameter is formally defined as

$$q = -1 - \frac{\dot{H}}{H^2} = -1 + \frac{d}{dt}\left(\frac{1}{H}\right), \tag{21}$$

and, using the parametrized Hubble function in Equation (20), we derive

$$q(z) = -1 + \frac{\alpha\beta(1+z)^{\beta}}{2\left[\alpha(1+z)^{\beta} + (1-\alpha)\right]}. \tag{22}$$

4. Datasets and Observational Framework

BAO refer to the periodic fluctuations imprinted on the photon-baryon plasma during the drag epoch. They arise from acoustic waves in the early universe. These fluctuations are set at the sound horizon scale r_d at the epoch of recombination (z_d∼1060). They provide a robust cosmological standard ruler for measuring cosmic distances and probing the expansion history of the universe. Unlike constraints from the CMB or SNe Ia, BAO mea-

surements offer an independent avenue for constraining cosmological parameters [52,53]. The BAO feature is identified across various astrophysical tracers and redshift ranges. The BOSS survey, for example, utilizes the correlation function of Lyman-α absorption lines from quasar spectra, as well as galaxy clustering of luminous red galaxies, emission-line galaxies, and quasars to detect the BAO signature [54,55]. The BAO scale, observable at multiple redshifts, reflects the integrated expansion of the universe since recombination, making it instrumental for constraining late-time cosmology.

In this analysis, we incorporate BAO measurements from a wide range of sources, including SDSS, WiggleZ, DECaLS, DES, and 6dFGS [56–70]. Additionally, we utilize CC data [71–74], which provide direct, model-independent measurements of the Hubble parameter $H(z)$ based on the differential aging of galaxies. We also include the Pantheon sample of SNe Ia [1,75–77], complemented by high-redshift probes such as quasars [78] and gamma-ray bursts [79].

To relate these observables to cosmological theory, several distance measures are introduced. The comoving angular diameter distance is defined as

$$D_M(z) = \frac{c}{H_0} \int_0^z \frac{dz'}{E(z')}, \tag{23}$$

where $E(z) = H(z)/H_0$ is the dimensionless Hubble parameter. From this, the angular diameter distance $D_A(z) = D_M(z)/(1+z)$ and the Hubble distance $D_H(z) = c/H(z)$ can be derived. A commonly used quantity in BAO analyses is the volume-averaged distance, defined as

$$D_V(z) = \left[z D_H(z) D_M^2(z) \right]^{1/3}. \tag{24}$$

The sound horizon at the drag epoch, which sets the BAO scale, is given by

$$r_d = \int_1^{z_d} \frac{c_s(z)}{H(z)} dz, \tag{25}$$

where $c_s(z)$ is the sound speed in the photon-baryon fluid, approximated by

$$c_s(z) \approx \frac{c}{\sqrt{3\left(1 + \frac{3\Omega_b(z)}{4\Omega_\gamma(z)}\right)}}. \tag{26}$$

In practice, BAO measurements yield the angular and redshift projections

$$\theta_z = \frac{r_d H(z)}{c}, \quad \theta_\ell = \frac{r_d}{(1+z) D_A(z)},$$

which imply that BAO data constrain the combination $r_d H(z)$ rather than r_d and $H(z)$ individually. To disentangle these quantities, an independent constraint on either H_0 or r_d is necessary.

To account for potential correlations among BAO measurements, we perform a covariance analysis as detailed in [80]. The covariance matrix for uncorrelated data points, $C_{aa} = \sigma_a^2$, is modified to include off-diagonal terms:

$$C_{ab} = \sigma_a \sigma_b (1 + \delta_{ab}), \quad \text{for } a \neq b, \tag{27}$$

where $\delta_{ab} = 0.5$ represents a 25% level of random correlation. Our analysis shows that introducing such correlations affects the final parameter estimates by less than 10%, confirming the robustness of treating these measurements as effectively uncorrelated.

Figures 1–3 collectively illustrate the effectiveness of our model in fitting the current observational data. Figure 1 shows the allowed confidence contours for model parameters, while Figure 2 confirms agreement between our model and $H(z)$ measurements, particularly at low redshifts. Figure 3 highlights the degeneracy between H_0 and r_d, a key factor in the ongoing Hubble tension. The robustness of our model across various datasets reinforces its suitability for late-time cosmological analyses.

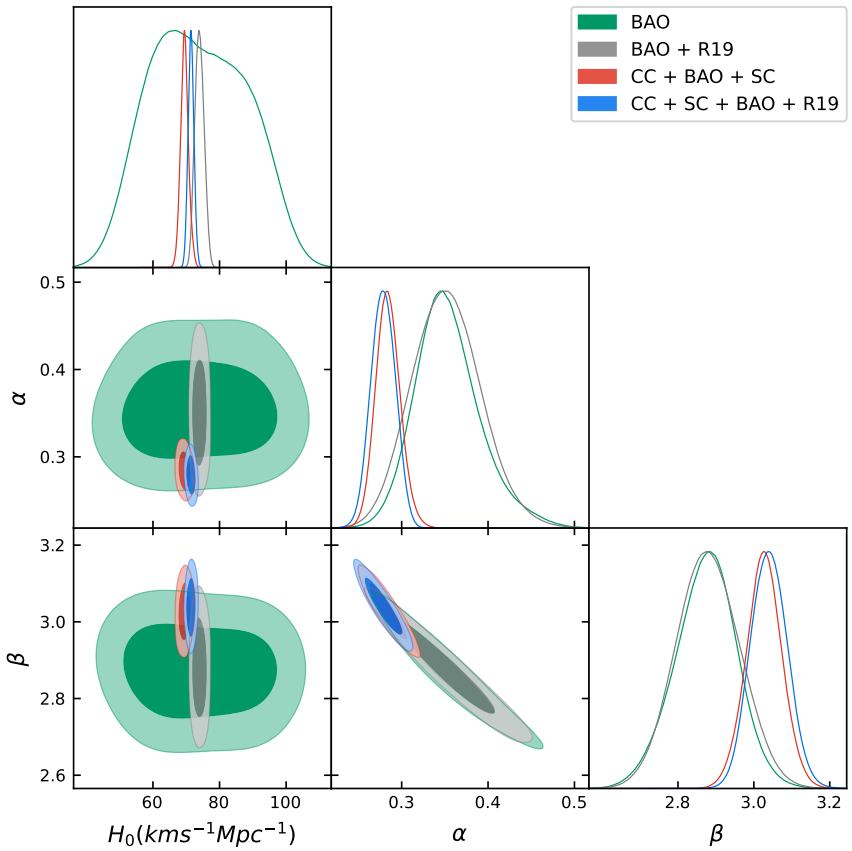

Figure 1. Confidence contours (1σ and 2σ) for model parameters obtained from various datasets.

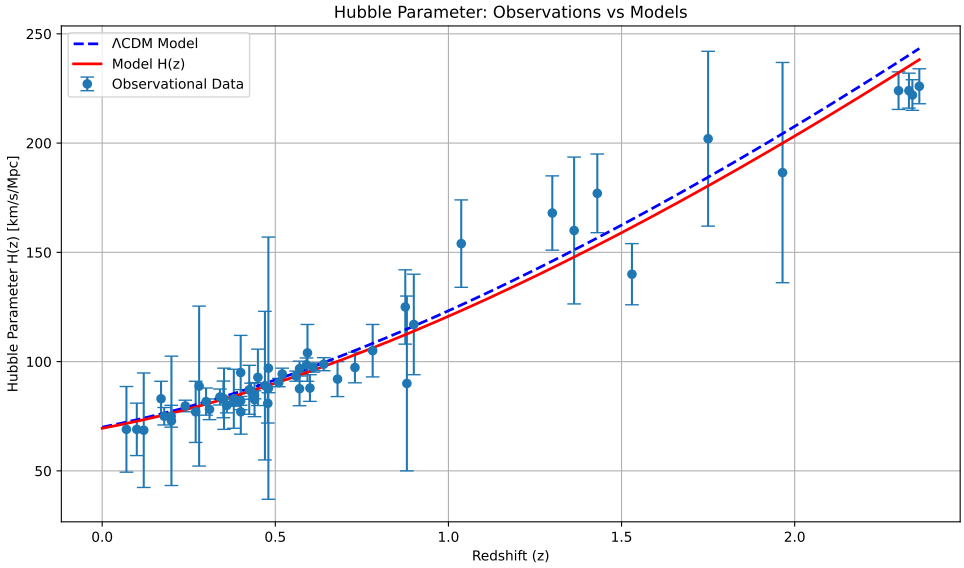

Figure 2. The Hubble parameter $H(z)$ as a function of redshift z for our model (solid line), compared with observational data and the ΛCDM model (dotted line).

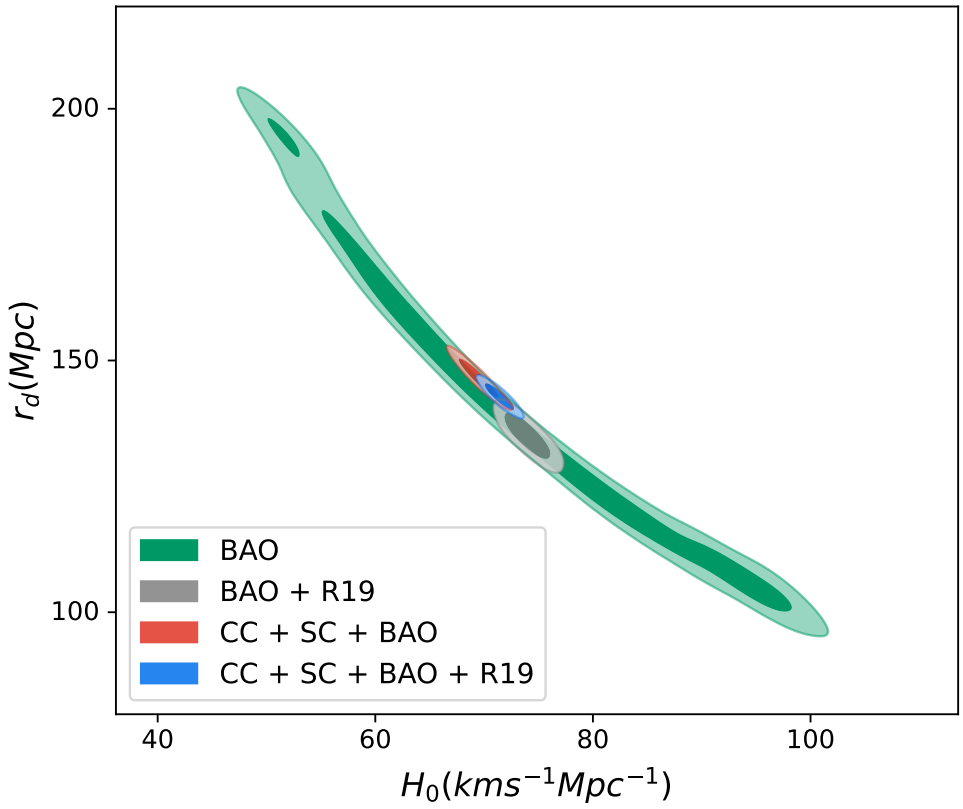

Figure 3. Correlation between the sound horizon scale r_d and the Hubble constant H_0 for various dataset combinations.

Whilst we have used BAO data to constrain the parameters of our model, we now explain briefly why we cannot use CMB data to do the same. In this work, we are concerned with the late-time expansion of the universe, not early-universe behavior needed for CMB analysis. We have examined in detail whether the phenomenological expansion model used in this work can accommodate CMB observations. The present model does not include radiation or early-universe components, and, therefore, a proper CMB analysis cannot be performed without modifying the underlying functional form of H(z) as given in Equation (20). This is a valid and widely accepted rationale, especially for models constructed specifically for late-time cosmology. At recombination ($z\sim1100$), the true expansion rate is dominated by matter and radiation

$$H^2(z) \sim (1+z)^4 + (1+z)^3 + (1+z)^2 + \ldots,$$

whereas our model contains only a single power-law term $(1+z)^\beta$. No single choice of parameter in the range $[2,4]$ can mimic both the radiation and matter contributions simultaneously. Hence, the Hubble function considered here is well suited for describing the late-time expansion of the universe but does not possess the correct early-universe behaviour needed for CMB analysis. Consequently, meaningful CMB fits would require extending the model, e.g., by incorporating a radiation-like term or a more complete early-time formulation. This is a topic for further investigation.

5. Cosmographic Parameters

To extract model-independent information about the universe's kinematic evolution, we analyze the cosmographic parameters, viz., the deceleration, jerk, and snap, which characterize the expansion history without assuming a specific gravitational theory. These

parameters are derived directly from derivatives of the scale factor $a(t)$ and are instrumental in probing the nature of cosmic acceleration.

5.1. Deceleration Parameter

The deceleration parameter $q(z)$ quantifies the rate of cosmic acceleration and was defined in Equation (21). Figure 4 depicts the reconstructed evolution of $q(z)$. Our analysis reveals a transition redshift $z_{\rm tr} \approx 0.68$, marking the epoch at which the universe shifted from decelerated to accelerated expansion. This aligns closely with the ΛCDM prediction $z_{\rm tr} \approx 0.67$ [3] (Planck 2018). At the present epoch ($z = 0$), the best-fit value $q_0 \approx -0.59$ also agrees well with the standard value $q_0 \approx -0.55$, supporting the validity of our parameterization. Small deviations may reflect dataset-specific systematics or manifestations of the H_0 tension, an ongoing debate in modern cosmology. We notice that, as the redshift approaches -1, q also approaches -1, as is the case with the ΛCDM model.

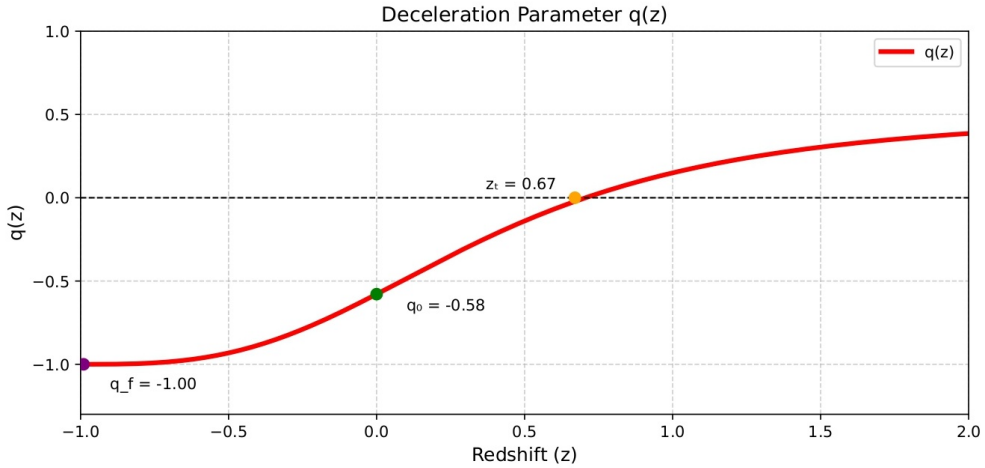

Figure 4. Reconstructed deceleration parameter $q(z)$. The transition from deceleration to acceleration occurs around $z_{\rm tr} \approx 0.68$.

5.2. Jerk Parameter

The jerk parameter $j(z)$ measures the third-order time derivative of the scale factor and provides a test for the ΛCDM model, for which j is a constant and $j = 1$. It is defined by

$$j(t) = \frac{\dddot{a}}{aH^3} = q(2q+1) + (1+z)\frac{dq}{dz}.$$

as a function of time t, and as a function of the redshift z, it is

$$j(z) = \left[-1 + \frac{\alpha\beta(1+z)^\beta}{2\left[\alpha(1+z)^\beta + (1-\alpha)\right]}\right]\left[1 + \frac{\alpha\beta(1+z)^\beta}{\left[\alpha(1+z)^\beta + (1-\alpha)\right]}\right] + \left[\frac{\alpha\beta^2(1+z)^\beta(1+z)^\beta}{2\left[\alpha(1+z)^\beta + (1-\alpha)\right]^2}\right]$$

As shown in Figure 5, our model predicts $j(z) > 1$, with the difference from the ΛCDM model decreasing with time. This deviation suggests the presence of a time-varying dark energy component or modification to GR. Specifically, we obtain $j_0 \approx 1.01$ at $z = 0$, indicating a slight departure from the constant ΛCDM value. In the future, $j(z)$ approaches the ΛCDM value 1 as $z \to -1$.

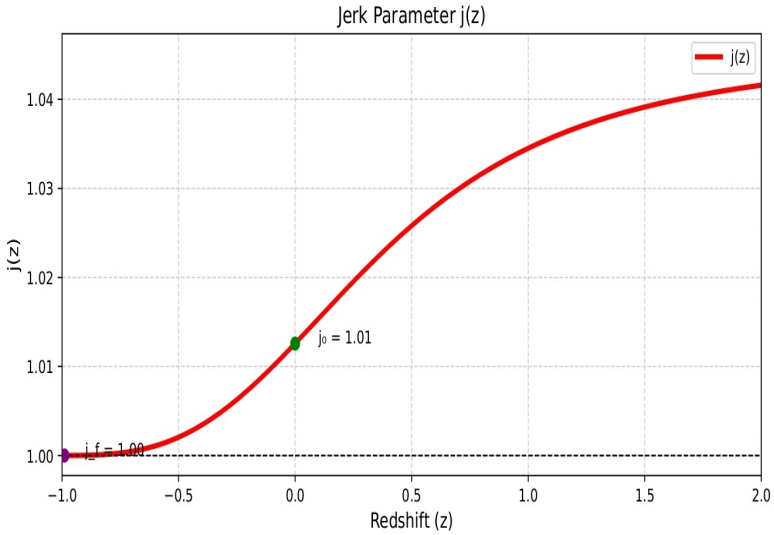

Figure 5. Redshift evolution of the jerk parameter $j(z)$. The slight deviation from the ΛCDM value ($j = 1$) suggests possible non-standard cosmological dynamics.

5.3. Snap Parameter

The snap parameter $s(z)$ probes the fourth derivative of the scale factor and offers insights into higher-order corrections in the expansion history. It is given by

$$s(z) = -\Big[-1 + \frac{3\alpha\beta(1+z)^{\beta}}{2\big[\alpha(1+z)^{\beta} + (1-\alpha)\big]}\Big]$$

This parameter is especially relevant in precision cosmology and helps to distinguish fine deviations from the ΛCDM scenario. Figure 6 presents the evolution of $s(z)$. Whilst our results broadly follow the trend expected from the ΛCDM model at lower redshifts, they also exhibit potential departures at $z < 0$, hinting at richer dynamical features beyond the standard paradigm. These deviations, though subtle, could signal evolving dark energy or higher-order gravitational effects.

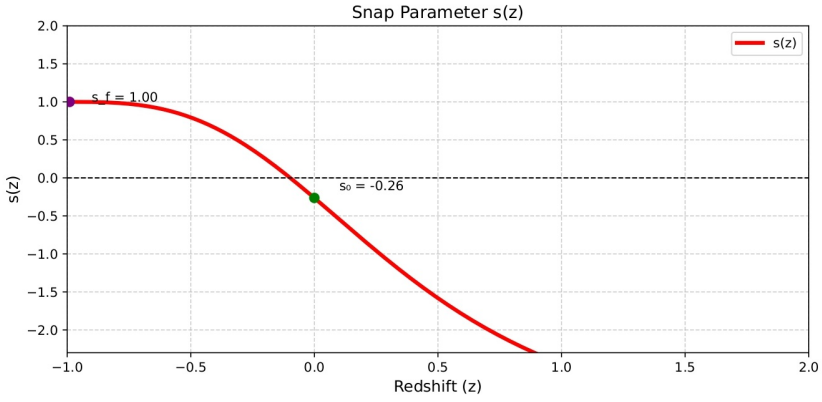

Figure 6. Reconstruction of the snap parameter $s(z)$ over redshift. The trajectory generally aligns with ΛCDM at low redshifts, with possible divergence as we go back in time.

6. Physical Characteristics of Quintessence as a Dark Energy Source: Cosmic Evolution

The equations of motion for a minimally coupled quintessence field can be derived using Equations (11) and (12), yielding expressions for the energy density and pressure of the scalar field as

$$M_{\rm Pl}^{-2}\rho^{\phi} = 3H^2 - M_{\rm Pl}^{-2}\rho^{m}, \tag{28}$$

$$M_{\rm Pl}^{-2}p^{\phi} = (2q-1)H^2, \tag{29}$$

under the assumption of pressureless matter ($p^m = 0$). We consider a two-component, non-interacting cosmic fluid: matter and the quintessence scalar field. The respective conservation equations take the form:

$$\dot{\rho}^m + 3H\rho^m = 0, \qquad \dot{\rho}^{\phi} + 3H(\rho^{\phi} + p^{\phi}) = 0. \tag{30}$$

Solving the matter conservation equation leads to

$$\rho^m = \rho_0 a^{-3} = \rho_0(1+z)^3, \tag{31}$$

where $\rho_0 = 3M_{\rm Pl}^2 H_0^2 \Omega_0^m$ denotes the present-day matter density. Substituting this back yields:

$$\rho^m = 3M_{\rm Pl}^2 H_0^2 \Omega_0^m (1+z)^3. \tag{32}$$

Using Equation (20), the scalar field energy density and pressure can be explicitly written as

$$M_{\rm Pl}^{-2}H_0^{-2}\rho^{\phi}(z) = 3\Big[\alpha(1+z)^{\beta} + 1 - \alpha\Big] - \rho_0(1+z)^3, \tag{33}$$

$$M_{\rm Pl}^{-2}H_0^{-2}p^{\phi}(z) = \left[-3 + \frac{\alpha\beta(1+z)^{\beta}}{\big[\alpha(1+z)^{\beta} + 1 - \alpha\big]}\right]\Big[\alpha(1+z)^{\beta} + 1 - \alpha\Big]. \tag{34}$$

In the figures below, we plot the energy density, pressure and EoS of the scalar field.

Figures 7–9 collectively demonstrate the viability of quintessence as a dark energy candidate. We see that the energy density is a positive monotonically decreasing function. The pressure is negative at late times, consistent with cosmological acceleration. Notably, the present-day value of the EoS parameter is $\omega_0^{\phi} \approx -0.8$, consistent with observational expectations for a slowly evolving dark energy component. In future, $\omega_0^{\phi} \to -1$, coinciding with the value for the ΛCDM model. It is notable that latest observations from DESI DR2 [81] seem to indicate an evolving EoS .

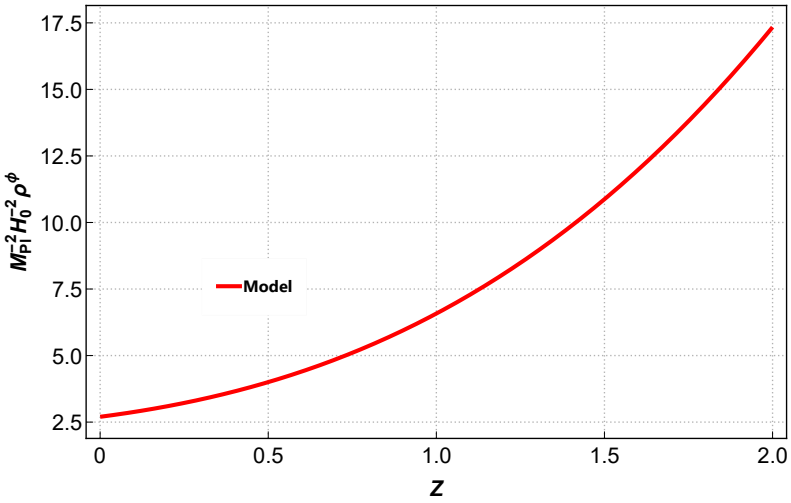

Figure 7. Normalized scalar field energy density $\rho^{\phi}(z)$ reconstructed using best-fit parameters from observational datasets.

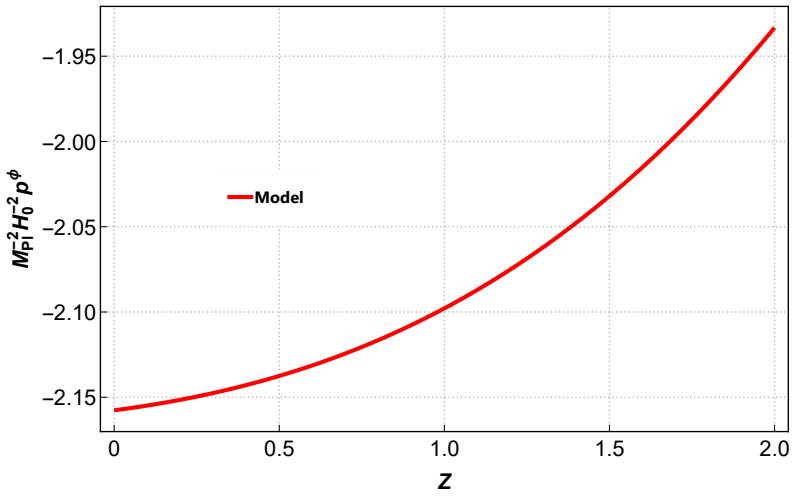

Figure 8. Normalized pressure $p^{\phi}(z)$ showing negative values across redshifts, essential for driving cosmic acceleration.

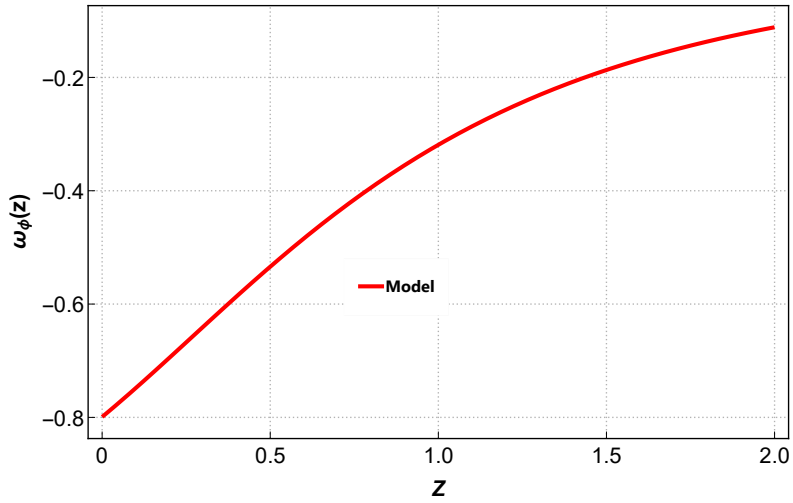

Figure 9. Evolution of the scalar field EoS $\omega^{\phi}(z) = p^{\phi}/\rho^{\phi}$, remaining within the quintessence range $-1 < \omega^{\phi} < 0$.

Kinetic and Potential Terms of the Scalar Field

The dynamics of the quintessence field are determined by its kinetic energy $\dot{\phi}^2$ and potential $V(\phi)$. Using Equations (17), (18), and (31), we express these quantities as

$$\dot{\phi}^2 = 2M_{\rm Pl}^2 H_0^2 \frac{\alpha\beta(1+z)^{\beta}}{2\left[\alpha(1+z)^{\beta}+1-\alpha\right]}\left[\alpha(1+z)^{\beta}+1-\alpha\right] - \rho_0(1+z)^3, \tag{35}$$

$$V(z) = M_{\rm Pl}^2 H_0^2 \left[1 - \frac{\alpha\beta(1+z)^{\beta}}{2\left[\alpha(1+z)^{\beta}+1-\alpha\right]}\right]\left[\alpha(1+z)^{\beta}+1-\alpha\right] - \frac{\rho_0}{2}(1+z)^3. \tag{36}$$

To reconstruct the potential $V(\phi)$ in physically meaningful terms, we transform the redshift-dependent quantities into scalar field-dependent ones. By numerically integrating $\dot{\phi}$ via

$$\frac{d\phi}{dz} = \frac{\dot{\phi}}{(1+z)H(z)},$$

we obtain $\phi(z)$, which enables us to plot the parametric form $V(\phi)$.

The monotonic evolution of $\phi(z)$ in Figure 10 confirms the scalar field's regular behavior across cosmic time, ensuring physical consistency. The resulting potential $V(\phi)$ in

Figure 11 shows a smooth, decreasing profile that flattens at early times –characteristic of viable quintessence models. This flattening allows the scalar field to slow-roll, mimicking a near-constant EoS as observed in Figure 9, thus providing a natural mechanism for late-time acceleration.

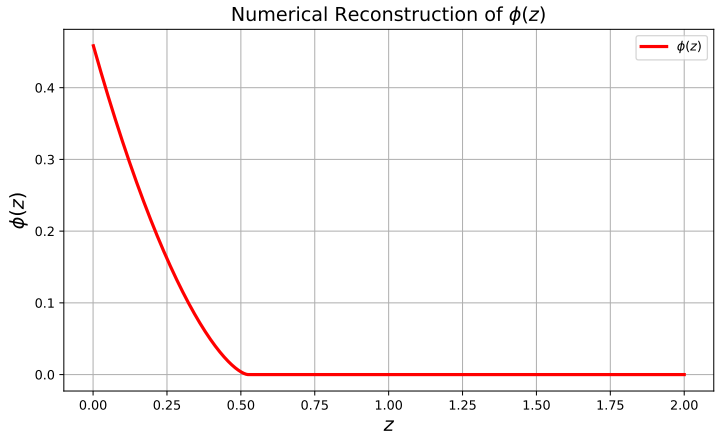

Figure 10. Evolution of the scalar field $\phi(z)$ reconstructed via numerical integration.

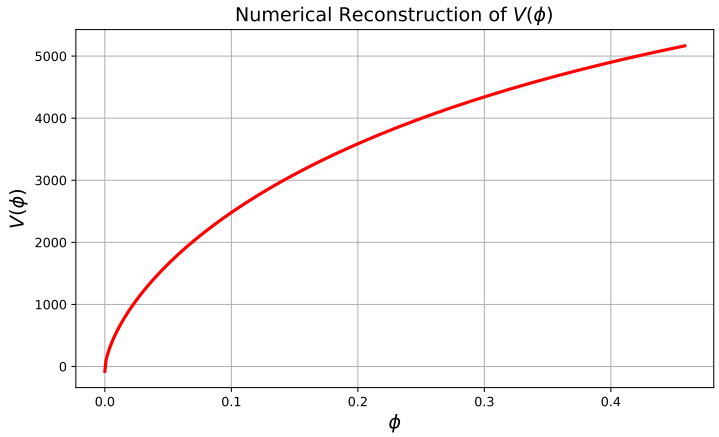

Figure 11. Reconstructed scalar potential $V(\phi)$, exhibiting a monotonic flattening behavior consistent with slow-roll quintessence dynamics.

7. Conclusions

In this work, we studied the late time acceleration of the universe via a scalar field cosmological model. Scalar fields provide a well-motivated class of models, which enable us to understand the current acceleration of the universe. Such fields have several advantages over the ΛCDM model. The model exbibits quintessence at late times, thus reducing the need for unnatural initial conditions. Especially chosen potentials, like the one here, allows the energy density of the scalar field to evolve and approach the matter density at late times, offering a solution to the coincidence problem. By a strategic choice of the Hubble parameter, we capture the key features that allow confrontation with observations.

After introducing the field equations entailing the scalar field, we adopted the parametrisation of the Hubble parameter as in Equation (19), which included the parameters H_0, α and β. We were then able to find $H(z)$ and $q(z)$. The latest observational datasets allowed a determination of these parammeters, as well as the sound horizon r_d at the drag epoch. The results from Table 1 show good agreement with those of the ΛCDM model. The cosmographic parameters, such as the deceleration, jerk and snap parameters were then studied and plotted against the redshift in Figures 4–6. We note from Figure 4 that $q_0 = -0.58$, and $z_t = 0.67$, in excellent agreement with the ΛCDM model.

The jerk parameter shows a small deviation from the ΛCDM value of $j = 1$ in the past but asymptotically approaches it in the future. The snap parameter aligns well with the ΛCDM curve at low redshifts, especially into the future, and deviates slightly going back into the past.

Table 1. The 95% confidence level constraints on the cosmological parameters for the ΛCDM model and our model for different combinations of the datasets.

MCMC Results						
Model	**Parameters**	**Priors**	**BAO**	**BAO + R19**	**CC + BAO + SC**	**CC + SC + BAO + R19**
ΛCDM Model	H_0	[50, 100]	$69.08^{+4.39}_{-6.25}$	$73.90^{+1.35}_{-2.78}$	$69.85^{+1.25}_{-2.38}$	$71.61^{+1.00}_{-1.93}$
	Ω_m	[0, 1]	$0.25^{+0.02}_{-0.06}$	$0.25^{+0.02}_{-0.06}$	$0.26^{+0.01}_{-0.02}$	$0.26^{+0.01}_{-0.03}$
	Ω_Λ	[0, 1]	$0.73^{+0.02}_{-0.03}$	$0.73^{+0.02}_{-0.06}$	$0.72^{+0.00}_{-0.01}$	$0.72^{+0.00}_{-0.01}$
	r_d	[100, 200]	$149.50^{+10.03}_{-15.21}$	$139.44^{+2.91}_{-5.88}$	$146.54^{+2.59}_{-5.01}$	$143.29^{+2.21}_{-4.35}$
	$r_d/r_{d,fid}$	[0.9, 1.1]	$1.00^{+0.06}_{-0.10}$	$0.94^{+0.02}_{-0.03}$	$0.99^{+0.01}_{-0.03}$	$0.96^{+0.01}_{-0.03}$
Proposed Model	H_0	[50, 100]	$73.74^{+5.61}_{-2.70}$	$73.98^{+1.35}_{-2.34}$	$69.48^{+1.15}_{-2.28}$	$71.43^{+0.87}_{-1.61}$
	α	[0, 0.6]	$0.353^{+0.033}_{-0.062}$	$0.351^{+0.04}_{-0.06}$	$0.284^{+0.013}_{-0.027}$	$0.278^{+0.01}_{-0.02}$
	β	[2, 4]	$2.873^{+0.07}_{-0.17}$	$2.879^{+0.07}_{-0.16}$	$3.02^{+0.04}_{-0.09}$	$3.03^{+0.04}_{-0.08}$
	r_d	[100, 200]	$140.66^{+31.47}_{-38.49}$	$135.03^{+2.86}_{-5.66}$	$146.54^{+2.32}_{-4.90}$	$142.79^{+1.63}_{-3.37}$
	$r_d/r_{d,fid}$	[0.9, 1.1]	$1.005^{+0.07}_{-0.1}$	$0.99^{+0.06}_{-0.09}$	$0.996^{+0.06}_{-0.09}$	$1.003^{+0.06}_{-0.09}$

We then considered the quintessence field to be minimally coupled, and pressure-less matter. The matter and scalar field were taken to be conserved independently, leading to expressions for the scalar density and pressure. These were plotted against the redshift, as well as the EoS. These exhibited the familiar characteristics of a monotonically decreasing energy density, negative pressure at late times, and the evolving EoS, which approaches the ΛCDM value of -1 in the future. The kinetic energy and potential of the scalar field were then determined, and numerically plotted. The field starts off being nearly constant at early times and starts increasing at late times from around $z = 0.5$.

To summarize, we have developed a generalized scalar-field extension of the ΛCDM model that allows controlled deviations in the cosmic expansion history while remaining fully compatible with dynamical scalar-field frameworks. This parametrized modification of $H(z)$ provides a new theoretical avenue for exploring dark energy behavior. To robustly test the model, we performed a comprehensive multi-probe MCMC analysis of CC, BAO, Pantheon SNe Ia, Quasars, and GRBs. This unified five-dataset approach represents a methodological advancement, enabling tighter and more reliable constraints on the underlying dynamics.

Our results reveal a transition redshift of $z_{\rm tr} = 0.69$ and a present-day deceleration parameter $q_0 = -0.64$, consistent with a quintessence-like EoS lying between -1 and 0. The model closely reproduces ΛCDM behavior at low redshifts but exhibits meaningful departures at $z \gtrsim 0.65$, leading to a slightly higher inferred value of H_0. This indicates that the proposed scalar-field extension may offer a partial alleviation of the Hubble tension through modified early-time expansion. However, this remains to be fully explored.

Overall, the work presents several key original contributions: (i) A new scalar-field generalization of the ΛCDM model. (ii) A joint five-probe MCMC constraint strategy not previously applied to such models. (iii) New physical insights connecting early-time deviations in $H(z)$ to a potential reduction in the H_0 and $H_0 - r_d$ tensions. (iv) Horndeski theories encompass a large number of free functions and couplings, making the resulting models powerful but difficult to constrain fully without strong theoretical priors and exten-

sive datasets. In contrast, the present work focuses on a minimal and phenomenological scalar-field extension of the ΛCDM model, constructed directly at the level of the background expansion. Our model does not attempt to explore the full Horndeski or DHOST function space; rather, it provides a controlled, observationally driven deviation from the ΛCDM model that retains compatibility with standard scalar-field dynamics. This allows us to focus on the cosmological consequences of a dynamical equation-of-state evolution without invoking the broader complexity of the full Horndeski class. (v) Directions towards a partial resolution to the Hubble tension problem.

Taken together, all the results reinforce the consistency of this scalar field model with present-day observations and its potential to act as a physically motivated alternative to the Λ, as well as with the potential to solve some of the issues with the ΛCDM model, e.g., the fine tuning and coincidence problems.

Funding: Aroonkumar Beesham is grateful to the DSTI-NRF Centre of Excellence in Mathematical and Statistical Sciences (CoE-MaSS), South Africa, for funding.

Data Availability Statement: No new data were created or analyzed in this study. Data sharing is not applicable to this article.

Acknowledgments: Opinions expressed and conclusions arrived at are those of the author and are not necessarily to be attributed to the CoE-MaSS. The author acknowledges the reviewers' comments, which have helped to improve the manuscript substantially.

Conflicts of Interest: The author declares no conflicts of interest.

References

1. Riess, A.G.; Filippenko, A.V.; Challis, P.; Clocchiatti, A.; Diercks, A.; Garnavich, P.M.; Gilliland, R.L.; Hogan, C.J.; Jha, S.; Kirshner, R.P.; et al. Observational evidence from supernovae for an accelerating universe and a cosmological constant. *Astron. J.* **1998**, *116*, 1009. [CrossRef]
2. Perlmutter, S.; Aldering, G.; Goldhaber, G.; Knop, R.A.; Nugent, P.; Castro, P.G.; Deustua, S.; Fabbro, S.; Goobar, A.; Groom, D.E.; et al. Measurements of Ω and Λ from 42 high-redshift supernovae. *Astrophys. J.* **1999**, *517*, 565–586. [CrossRef]
3. Collaboration, P. Planck 2018 results. VI. Cosmological parameters. *Astron. Astrophys.* **2020**, *641*, A6. [CrossRef]
4. Riess, A.G.; Macri, L.M.; Hoffmann, S.L.; Scolnic, D.; Casertano, S.; Filippenko, A.V.; Tucker, B.E.; Reid, M.J.; Jones, D.O.; Silverman, J.M.; et al. A 2.4% determination of the local value of the Hubble constant. *Astrophys. J.* **2016**, *826*, 56. [CrossRef]
5. Riess, A.G.; Casertano, S.; Yuan, W.; Bowers, J.B.; Macri, L.; Zinn, J.C.; Scolnic, D. Cosmic distances calibrated to 1% precision with Gaia EDR3 parallaxes and Hubble Space Telescope photometry of 75 Milky Way Cepheids confirm tension with ΛCDM. *Astrophys. J. Lett.* **2021**, *908*, L6. [CrossRef]
6. Aylor, K.; Joy, M.; Knox, L.; Millea, M.; Raghunathan, S.; Story, K. Sounds Discordant: Classical distance ladder and ΛCDM–based determinations of the cosmological sound horizon. *Astrophys. J.* **2019**, *874*, 4. [CrossRef]
7. Knox, L.; Millea, M. Hubble constant hunter's guide. *Phys. Rep.* **2021**, *913*, 1–65. [CrossRef]
8. Appleby, S.; Battye, R. Do Consistent $F(R)$ Models Mimic General Relativity plus Lambda? *Phys. Lett. B* **2007**, *654*, 7–12. [CrossRef]
9. Amendola, L.; Gannouji, R.; Polarski, D.; Tsujikawa, S. Conditions for the cosmological viability of $f(R)$ dark energy models. *Phys. Rev. D.* **2007**, *75*, 083504. [CrossRef]
10. Saffari, R.; Rahvar, S. Consistency Condition of Spherically Symmetric Solutions in $f(R)$ Gravity. *Phys. Rev. D.* **2008**, *77*, 104028. [CrossRef]
11. Nashe, G. Energy Conditions of Built-In Inflation Models in $f(T)$ Gravitational Theories. *Gen. Relativ. Gravit.* **2015**, *47*, 1–14.
12. Setare, M.; Mohammadipour, N. Can $f(T)$ gravity theories mimic ΛCDM cosmic history. *J. Cosmol. Astropart. Phys.* **2013**, *2013*, 015. [CrossRef]
13. Harko, T.; Lobo, F.S.N.; Nojiri, S.; Odintsov, S.D. $f(R,T)$ gravity. *Phys. Rev. D.* **2011**, *84*, 024020. [CrossRef]
14. Sahlu, S.; Alfedeel, A.H.A.; Abebe, A. The cosmology of $f(R,L_m)$ gravity: Constraining the background and perturbed dynamics. *arXiv* **2024**, arXiv:2406.08303.
15. Jiménez, J.B.; Heisenberg, L.; Koivisto, T. Coincident general relativity. *Phys. Rev. D* **2018**, *98*. [CrossRef]
16. Jiménez, J.B.; Heisenberg, L.; Koivisto, T.; Pekar, S. Cosmology in $f(Q)$ geometry. *Phys. Rev. D* **2020**, *101*, 103507. [CrossRef]
17. Xu, Y.; Li, G.; Harko, T.; Liang, S.D. $f(Q,T)$ gravity. *Eur. Phys. J. C* **2019**, *79*, 708. [CrossRef]

18. Horndeski, G.W. Second-Order Scalar-Tensor Field Equations in a Four-Dimensional Space. *Int. J. Theor. Phys.* **1974**, *10*, 363–384. [CrossRef]
19. Langlois, D. Dark energy and modified gravity in degenerate higher-order scalar–tensor (DHOST) theories: A review. *Int. J. Mod. Phys. D* **2019**, *28*, 1942006. [CrossRef]
20. Ratra, B.; Peebles, P.J.E. Cosmological consequences of a rolling homogeneous scalar field. *Phys. Rev. D* **1988**, *37*, 3406–3427. [CrossRef]
21. Copeland, E.J.; Sami, M.; Tsujikawa, S. Dynamics of Dark Energy. *Int. J. Mod. Phys. D* **2006**, *15*, 1753–1935. [CrossRef]
22. Zlatev, I.; Wang, L.; Steinhardt, P.J. Quintessence, Cosmic Coincidence, and the Cosmological Constant. *Phys. Rev. Lett.* **1999**, *82*, 896–899. [CrossRef]
23. Steinhardt, P.J.; Wang, L.; Zlatev, I. Cosmological tracking solutions. *Phys. Rev. D* **1999**, *59*, 123504. [CrossRef]
24. Johri, V.B. Genesis of cosmological tracker fields. *Phys. Rev. D* **2001**, *63*, 103504. [CrossRef]
25. Amendola, L.; Tocchini-Valentini, D. Stationary dark energy: The present universe as a global attractor. *Phys. Rev. D* **2001**, *64*, 043509. [CrossRef]
26. Gasperini, M.; Piazza, F.; Veneziano, G. Quintessence as a runaway dilaton. *Phys. Rev. D* **2001**, *65*, 023508. [CrossRef]
27. Armendariz-Picon, C.; Mukhanov, V.; Steinhardt, P.J. Dynamical Solution to the Problem of a Small Cosmological Constant and Late-Time Cosmic Acceleration. *Phys. Rev. Lett.* **2000**, *85*, 4438–4441. [CrossRef]
28. Boyle, L.A.; Caldwell, R.R.; Kamionkowski, M. Spintessence! New models for dark matter and dark energy. *Phys. Lett. B* **2002**, *545*, 17–22. [CrossRef]
29. Jawad, A.; Majeed, A. Correspondence of pilgrim dark energy with scalar field models. *Astrophys. Space Sci.* **2015**, *356*, 375–381. [CrossRef]
30. Chiba, T.; Okabe, T.; Yamaguchi, M. Kinetically driven quintessence. *Phys. Rev. D* **2000**, *62*, 023511. [CrossRef]
31. Sadjadi, H.M.; Alimohammadi, M. Transition from quintessence to the phantom phase in the quintom model. *Phys. Rev. D* **2006**, *74*, 043506. [CrossRef]
32. Ade, P.A.R.; Aghanim, N.; Arnaud, M.; Ashdown, M.; Aumont, J.; Baccigalupi, C.; Banday, A.J.; Barreiro, R.B.; Bartolo, N.; Battaner, E.; et al. Planck2015 results: XXVIII. ThePlanckCatalogue of Galactic cold clumps. *Astron. Astrophys.* **2016**, *594*, A28.
33. Kamenshchik, A.; Moschella, U.; Pasquier, V. An alternative to quintessence. *Phys. Lett. B* **2001**, *511*, 265–268. [CrossRef]
34. Shafieloo, A.; Kim, A.G.; Linder, E.V. Gaussian process cosmography. *Phys. Rev. D* **2012**, *85*, 123530. [CrossRef]
35. Shafieloo, A.; Kim, A.G.; Linder, E.V. Model independent tests of cosmic growth versus expansion. *Phys. Rev. D* **2013**, *87*, 023520. [CrossRef]
36. Dinda, B.R. Model independent parametrization of the late time cosmic acceleration: Constraints on the parameters from recent observations. *Phys. Rev. D* **2019**, *100*, 043528. [CrossRef]
37. Corasaniti, P.S.; Copeland, E.J. Model independent approach to the dark energy equation of state. *Phys. Rev. D* **2003**, *67*, 063521. [CrossRef]
38. Riess, A.G.; Casertano, S.; Yuan, W.; Macri, L.M.; Scolnic, D. Large Magellanic Cloud Cepheid Standards Provide a 1% Foundation for the Determination of the Hubble Constant and Stronger Evidence for Physics beyond ΛCDM. *Ap. J.* **2019**, *876*, 85. [CrossRef]
39. Bouali, A.; Chaudhary, H.; Mehrotra, A.; Pacif, S.K.J. Model-independent study for a quintessence model of dark energy: Analysis and observational constraints. *Fortschritte Der Phys.* **2023**, *71*, 2300086. [CrossRef]
40. Zimdahl, W.; Pavón, D. Statefinder parameters for interacting dark energy. *Gen. Relativ. Gravit.* **2004**, *36*, 1483–1491. [CrossRef]
41. Bertolami, O.; Martins, P.J. Nonminimal coupling and quintessence. *Phys. Rev. D* **2000**, *61*, 064007. [CrossRef]
42. Banerjee, N.; Pavón, D. Cosmic acceleration without quintessence. *Phys. Rev. D* **2001**, *63*, 043504. [CrossRef]
43. Overduin, J.; Cooperstock, F. Evolution of the scale factor with a variable cosmological term. *Phys. Rev. D* **1998**, *58*, 043506. [CrossRef]
44. Saini, T.D.; Raychaudhury, S.; Sahni, V.; Starobinsky, A.A. Reconstructing the cosmic equation of state from supernova distances. *Phys. Rev. Lett.* **2000**, *85*, 1162. [CrossRef] [PubMed]
45. Simon, J.; Verde, L.; Jimenez, R. Constraints on the redshift dependence of the dark energy potential. *Phys. Rev. D—Part. Fields Gravit. Cosmol.* **2005**, *71*, 123001. [CrossRef]
46. Paul, S.; Das, R.K.; Pan, S. Parametrizing the Hubble function instead of dark energy: Many possibilities. *Phys. Rev. D* **2025**, *112*, 043542. [CrossRef]
47. Benisty, D.; Pan, S.; Staicova, D.; Valentino, E.D.; Nunes, R.C. Late-time constraints on interacting dark energy: Analysis independent of H0, rd, and MB. *Astron. Astrophys.* **2024**, *688*, A156. [CrossRef]
48. Pan, S.; Bhattacharya, S.; Chakraborty, S. An analytic model for interacting dark energy and its observational constraints. *Mon. Not. R. Astron. Soc.* **2015**, *452*, 3038–3046. [CrossRef]
49. Pan, S.; Sharov, G.S. A model with interaction of dark components and recent observational data. *Mon. Not. R. Astron. Soc.* **2017**, *472*, 4736–4749. [CrossRef]

50. He, T.Y.; Yin, J.J.; Wang, Z.Y.; Han, Z.W.; Yang, R.J. A new parametrization of Hubble function and Hubble tension. *J. Cosmol. Astropart. Phys.* **2024**, *2024*, 028. [CrossRef]
51. Sharov, G.S.; Bhattacharya, S.; Pan, S.; Nunes, R.C.; Chakraborty, S. A new interacting two-fluid model and its consequences. *Mon. Not. R. Astron. Soc.* **2016**, *466*, 3497–3506. [CrossRef]
52. Handley, W. Curvature tension: Evidence for a closed universe. *Phys. Rev. D* **2021**, *103*, L041301. [CrossRef]
53. Valentino, E.D.; Melchiorri, A.; Silk, J. Cosmic discordance: Planck and luminosity distance data exclude ΛCDM. *arXiv* **2020**, arXiv:2003.04935.
54. Cuceu, A.; Farr, J.; Lemos, P.; Font-Ribera, A. Baryon acoustic oscillations and the Hubble constant: Past, present and future. *J. Cosmol. Astropart. Phys.* **2019**, *2019*, 044. [CrossRef]
55. Wu, W.K.; Motloch, P.; Hu, W.; Raveri, M. Hubble constant difference between CMB lensing and BAO measurements. *Phys. Rev. D* **2020**, *102*, 023510. [CrossRef]
56. Beutler, F.; Blake, C.; Colless, M.; Jones, D.H.; Staveley-Smith, L.; Campbell, L.; Parker, Q.; Saunders, W.; Watson, F. The 6dF Galaxy Survey: Baryon acoustic oscillations and the local Hubble constant. *Mon. Not. R. Astron. Soc.* **2011**, *416*, 3017–3032. [CrossRef]
57. Ross, A.J.; Samushia, L.; Howlett, C.; Percival, W.J.; Burden, A.; Manera, M. The clustering of the SDSS DR7 main galaxy sample–I. A 4 per cent distance measure at $z = 0.15$. *Mon. Not. R. Astron. Soc.* **2015**, *449*, 835–847. [CrossRef]
58. Blazek, J.A.; McEwen, J.E.; Hirata, C.M. Streaming velocities and the baryon acoustic oscillation scale. *Phys. Rev. Lett.* **2016**, *116*, 121303. [CrossRef]
59. Pellejero-Ibanez, M.; Chuang, C.H.; Rubiño-Martín, J.; Cuesta, A.J.; Wang, Y.; Zhao, G.; Ross, A.J.; Rodríguez-Torres, S.; Prada, F.; Slosar, A.; et al. The clustering of galaxies in the completed SDSS-III Baryon Oscillation Spectroscopic Survey: Double-probe measurements from BOSS galaxy clustering & Planck data–towards an analysis without informative priors. *arXiv* **2016**, arXiv:1607.03152.
60. Blake, C.; Brough, S.; Colless, M.; Contreras, C.; Couch, W.; Croom, S.; Croton, D.; Davis, T.M.; Drinkwater, M.J.; Forster, K.; et al. The WiggleZ Dark Energy Survey: Joint measurements of the expansion and growth history at $z < 1$. *Mon. Not. R. Astron. Soc.* **2012**, *425*, 405–414.
61. Seo, H.J.; Ho, S.; White, M.; Cuesta, A.J.; Ross, A.J.; Saito, S.; Reid, B.; Padmanabhan, N.; Percival, W.J.; Putter, R.D.; et al. Acoustic scale from the angular power spectra of SDSS-III DR8 photometric luminous galaxies. *Astrophys. J.* **2012**, *761*, 13. [CrossRef]
62. Soumagnac, M.; Barkana, R.; Sabiu, C.; Loeb, A.; Ross, A.; Abdalla, F.; Balan, S.; Lahav, O. Large scale distribution of total mass versus luminous matter from baryon acoustic oscillations: First search in the SDSS-III BOSS data release 10. *arXiv* **2016**, arXiv:1602.01839. [CrossRef]
63. Sridhar, S.; Song, Y.S.; Ross, A.J.; Zhou, R.; Newman, J.A.; Chuang, C.H.; Blum, R.; Gaztanaga, E.; Landriau, M.; Prada, F. Clustering of LRGs in the DECaLS DR8 footprint: Distance constraints from baryon acoustic oscillations using photometric redshifts. *Astrophys. J.* **2020**, *904*, 69. [CrossRef]
64. Bautista, J.E.; Vargas-Magaña, M.; Dawson, K.S.; Percival, W.J.; Brinkmann, J.; Brownstein, J.; Camacho, B.; Comparat, J.; Gil-Marín, H.; Mueller, E.M.; et al. The SDSS-IV extended Baryon Oscillation Spectroscopic Survey: Baryon acoustic oscillations at redshift of 0.72 with the DR14 luminous red galaxy sample. *Astrophys. J.* **2018**, *863*, 110. [CrossRef]
65. Mena-Fernández, J.; Rodríguez-Monroy, M.; Avila, S.; Porredon, A.; Chan, K.; Camacho, H.; Weaverdyck, N.; Sevilla-Noarbe, I.; Sanchez, E.; Cipriano, L.T.S.; et al. Dark Energy Survey: Galaxy sample for the baryonic acoustic oscillation measurement from the final dataset. *Phys. Rev. D* **2024**, *110*, 063514. [CrossRef]
66. Hou, J.; Sánchez, A.G.; Ross, A.J.; Smith, A.; Neveux, R.; Bautista, J.; Burtin, E.; Zhao, C.; Scoccimarro, R.; Dawson, K.S.; et al. The completed SDSS-IV extended Baryon Oscillation Spectroscopic Survey: BAO and RSD measurements from anisotropic clustering analysis of the quasar sample in configuration space between redshift 0.8 and 2.2. *Mon. Not. R. Astron. Soc.* **2021**, *500*, 1201–1221. [CrossRef]
67. Busca, N.G.; Delubac, T.; Rich, J.; Bailey, S.; Font-Ribera, A.; Kirkby, D.; Goff, J.M.L.; Pieri, M.M.; Slosar, A.; Aubourg, É.; et al. Baryon acoustic oscillations in the Ly-α forest of BOSS quasars. *arXiv* **2012**, arXiv:1211.2616.
68. de Sainte Agathe, V.; Balland, C.; Bourboux, H.D.M.D.; Blomqvist, M.; Guy, J.; Rich, J.; Font-Ribera, A.; Pieri, M.M.; Bautista, J.E.; Dawson, K.; et al. Baryon acoustic oscillations at $z = 2.34$ from the correlations of Lyα absorption in eBOSS DR14. *Astron. Astrophys.* **2019**, *629*, A85. [CrossRef]
69. Carter, P.; Beutler, F.; Percival, W.J.; Blake, C.; Koda, J.; Ross, A.J. Low redshift baryon acoustic oscillation measurement from the reconstructed 6-degree Field Galaxy Survey. *Mon. Not. R. Astron. Soc.* **2018**, *481*, 2371–2383. [CrossRef]
70. Kazin, E.A.; Koda, J.; Blake, C.; Padmanabhan, N.; Brough, S.; Colless, M.; Contreras, C.; Couch, W.; Croom, S.; Croton, D.J.; et al. The WiggleZ Dark Energy Survey: Improved distance measurements to $z = 1$ with reconstruction of the baryonic acoustic feature. *Mon. Not. R. Astron. Soc.* **2014**, *441*, 3524–3542. [CrossRef]
71. Moresco, M.; Verde, L.; Pozzetti, L.; Jimenez, R.; Cimatti, A. New constraints on cosmological parameters and neutrino properties using the expansion rate of the Universe to $z\sim1.75$. *J. Cosmol. Astropart. Phys.* **2012**, *2012*, 053. [CrossRef]

72. Moresco, M.; Cimatti, A.; Jimenez, R.; Pozzetti, L.; Zamorani, G.; Bolzonella, M.; Dunlop, J.; Lamareille, F.; Mignoli, M.; Pearce, H.; et al. Improved constraints on the expansion rate of the Universe up to $z\sim1.1$ from the spectroscopic evolution of cosmic chronometers. *J. Cosmol. Astropart. Phys.* **2012**, *2012*, 006. [CrossRef]
73. Moresco, M. Raising the bar: New constraints on the Hubble parameter with cosmic chronometers at $z\sim2$. *Mon. Not. R. Astron. Soc. Lett.* **2015**, *450*, L16–L20. [CrossRef]
74. Moresco, M.; Pozzetti, L.; Cimatti, A.; Jimenez, R.; Maraston, C.; Verde, L.; Thomas, D.; Citro, A.; Tojeiro, R.; Wilkinson, D. A 6% measurement of the Hubble parameter at $z\sim0.45$: Direct evidence of the epoch of cosmic re-acceleration. *J. Cosmol. Astropart. Phys.* **2016**, *2016*, 014. [CrossRef]
75. Howell, D.A.; Sullivan, M.; Nugent, P.E.; Ellis, R.S.; Conley, A.J.; Borgne, D.L.; Carlberg, R.G.; Guy, J.; Balam, D.; Basa, S.; et al. The type Ia supernova SNLS-03D3bb from a super-Chandrasekhar-mass white dwarf star. *Nature* **2006**, *443*, 308–311. [CrossRef]
76. Scolnic, D.M.; Jones, D.; Rest, A.; Pan, Y.; Chornock, R.; Foley, R.; Huber, M.; Kessler, R.; Narayan, G.; Riess, A.; et al. The complete light-curve sample of spectroscopically confirmed SNe Ia from Pan-STARRS1 and cosmological constraints from the combined Pantheon sample. *Astrophys. J.* **2018**, *859*, 101. [CrossRef]
77. Anagnostopoulos, F.K.; Basilakos, S.; Saridakis, E.N. Observational constraints on Barrow holographic dark energy. *Eur. Phys. J. C* **2020**, *80*, 826. [CrossRef]
78. Roberts, C.; Horne, K.; Hodson, A.O.; Leggat, A.D. Tests of ΛCDM and conformal gravity using GRB and quasars as standard candles out to $z\sim8$. *arXiv* **2017**, arXiv:1711.10369.
79. Demianski, M.; Piedipalumbo, E.; Sawant, D.; Amati, L. Cosmology with gamma-ray bursts—I. The Hubble diagram through the calibrated $E_{p,i}$–E_{iso} correlation. *Astron. Astrophys.* **2017**, *598*, A112. [CrossRef]
80. Kazantzidis, L.; Perivolaropoulos, L. Evolution of the $f\sigma_8$ tension with the Planck15/ΛCDM determination and implications for modified gravity theories. *Phys. Rev. D* **2018**, *97*, 103503. [CrossRef]
81. Collaboration, D.; Abdul-Karim, M.; Aguilar, J.; Ahlen, S.; Alam, S.; Allen, L.; Prieto, C.A.; Alves, O.; Anand, A.; Andrade, U.; et al. DESI DR2 Results II: Measurements of Baryon Acoustic Oscillations and Cosmological Constraints. *Phys. Rev. D* **2025**, *112*, 083515. [CrossRef]